Environmental Modelling and Software 117 (2019) 29–42

Contents lists available at ScienceDirect

Environmental Modelling & Software

journal homepage: www.elsevier.com/locate/envsoft

Sensor web - Enabled flood event process detection and instant service

Wenying Du[a,b,c], Nengcheng Chen[a,d,*], Sai Yuan[a], Chao Wang[a], Min Huang[a], Huanfeng Shen[b]

[a] State Key Laboratory of Information Engineering in Surveying, Mapping and Remote Sensing, Wuhan University, Wuhan, Hubei, 430079, China
[b] School of Resource and Environmental Sciences, Wuhan University, Wuhan, Hubei, 430079, China
[c] Changjiang River Scientific Research Institute of Changjiang Water Resources Commission, Wuhan, Hubei, 430015, China
[d] Collaborative Innovation Center of Geospatial Technology, Wuhan University, Wuhan, Hubei, 430079, China

ARTICLE INFO

Keywords:
Flood
Detection and service
Full life cycle
Sensor web
Water level prediction

ABSTRACT

Flood Detection and Service (FD&S) is of great significance to flood management and decision-making. But most of the state-of-art FD&S methods are weak in timeliness and extensibility, and could not reflect flood processes. To resolve the abovementioned problems, this paper proposed the process-based FD&S (PFD&S) method based on Sensor Web. PFD&S is a four-layer architecture the core components of which are the access adapter and process-based detection rules and it is capable of heterogeneous sensor access, flood detection, and flood phase adaptive services. A prototype was developed based on the PFD&S method. Two floods occurring in the Huanghan basin (Hubei, China, with the area of 5.04×10^4 km^2) during July 2016, was selected as the case studies to validate the PFD&S method and prototype. The results demonstrated that the proposed PFD&S method and prototype could achieve the instant flood process detection and services in 2.7 min.

1. Introduction

Hydrological disasters took the largest share, 51.7%, in natural disasters occurrence worldwide in 2016, causing 5092 deaths, 78.1 million people reported affected, and damages totaling almost US$ 59 billion. Among the hydrological disasters, 92.7% were floods, with the total occurrence of 164 times worldwide. The total deaths, people reported affected, and damages of floods accounted for 92.9%, 99.7%, and 98.8% of the total hydrological disasters, respectively (Guha-Sapir et al., 2016). As the natural disaster type with the highest occurrence frequency and resulting in the most serious casualties and economic losses, the requirements for decreasing the life loss and property damage caused by floods are imperious all over the world (Hirsch and Archfield, 2015). Adequate preparations, effective warnings, and timely public responses are all of great significance to reduce the losses from flooding (Demir and Krajewski, 2013). The flood detection and service (FD&S) is exactly to detect floods in advance and provide the corresponding services, i.e., alert, therefore, it is of urgent need to conduct researches on FD&Ss.

There are many literature relevant to FD&Ss. According to the variable types, FD&S methods can be divided into Inundated Area - Based (IAB) (Dai et al., 2015; Sghaier et al., 2018), Submerged Depth - Based (SDB) (Gao et al., 2018), and Direct Observation Variables - Based (DOVB) detections, i.e., water level (Acosta-Coll et al., 2018), and precipitation (Darand and Sohrabi, 2018), etc. IAB flood detections can be mainly divided into two types, including the study of flooded area extraction algorithms (Cohen et al., 2016; Du et al., 2017a, 2017b; Liu et al., 2018) and the study of flood detection systems and applications (Auynirundronkool et al., 2012; Dai et al., 2015; Martinis and Rieke, 2015; Schlaffer et al., 2015; Mueller et al., 2016; Pekel et al., 2016; Amitrano et al., 2018; Cian et al., 2018; Giordan et al., 2018; Martinis et al., 2015; Sghaier et al., 2018; Tong et al., 2018; Veh et al., 2018).

The study of flood detection systems and applications includes the Global Flood Detection System (GFDS) (Revillaromero et al., 2014), the European Flood Alert System (EFAS) (Arnal et al., 2018), the Global Flood Awareness System (GloFAS) (Alfieri et al., 2013), and the Dartmouth Flood Observatory (DFO) (Reager and Famiglietti, 2009), etc. The data sources of IAB flood detections are usually satellite images. Satellite images have a wider spatial coverage which makes them suitable for flooded area determination, but the temporal resolution of remotely sensed data can be too low to acquire available data during floods when compared with ground observations. Crowdsourcing data were also used to determine flood ranges (Poser and Dransch, 2010; Fohringer et al., 2015; Witherow et al., 2017; Feng and Sester, 2018). But crowdsourcing data is the most dispersed data source and features high redundancy, thus it is often utilized as an auxiliary data sources for FD&S (Jongman et al., 2015).

* Corresponding author. State Key Laboratory of Information Engineering in Surveying, Mapping and Remote Sensing, Wuhan University, Wuhan, Hubei, 430079, China.
E-mail address: cnc@whu.edu.cn (N. Chen).

https://doi.org/10.1016/j.envsoft.2019.03.004
Received 25 December 2018; Accepted 6 March 2019
Available online 10 March 2019
1364-8152/

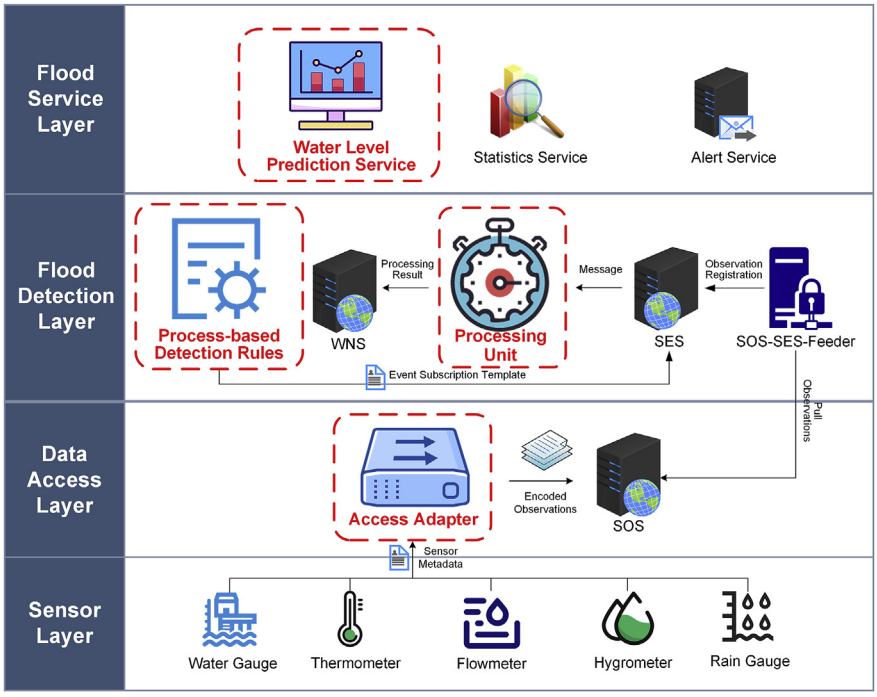

Fig. 1. Overall architecture of the PFD&S method.

SDB detection often simulates and analyzes the spatio - temporal variation of land surface runoff through hydrological or hydraulic models (Cane et al., 2013; Caruso et al., 2013; Moreno et al., 2013; Shi et al., 2015) to completes the FD&S. Detection accuracy of the SDB methods are usually relatively high via the repeated region - oriented process of iterative calculation and model parameter calibration. Although with high detection accuracy for specific areas, lots of manpower and computation resources should be invested before these regional detection models could be extended to other regions. Meanwhile the model simulation can be quite complicated with complex equations of mathematical physics and dozens of parameters, and it simultaneously puts forward high demands for historical observations and records. Therefore, it is quite difficult for SDB detections to be used for the flood detecting in regions lack of long time-series and comprehensive hydrological and meteorological data.

DOVB detection is usually implemented by threshold filtering of directly observed variables, i.e., water level (Acosta-Coll et al., 2018) or rainfall (Darand and Sohrabi, 2018). Ground observations with high temporal resolution ensure the timeliness of the DOVB detections, and make it suitable for the rapid detection and responding of floods (Acosta-Coll et al., 2018). But currently, this kind of methods mainly focus on the study of real-time sensor access and alert releasing for specific regions, and the universality and extensibility of the existing DOVB flood detections are often very poor, resulting in that they could not be reused in other regions or occasions easily. In addition, the most importantly, all the existing FD&S methods have the common defects, that is, they could only determine whether floods would occur or not at specific time instants, being unable to achieve the comprehensive understanding the whole process of flood occurrence and development.

In summary, for the rapid detection of floods occurring in the regions without adequate data support, the DOVB detection utilizing ground observation is more feasible and effective (Acosta-Coll et al., 2018). However, there are still mainly two problems faced with the existing DOVB detections utilizing ground observations: 1) the abovementioned common defects, the rapid full life cycle FD&S is absent, making it difficult to get a clear picture of the whole process of floods rapidly; 2) the universality and extensibility of FD&Ss are very low, with the same or similar problems repeatedly studied, resulting in a large amount of resource wastes. To solve the abovementioned two problems, the objective of this paper is: 1) propose a method to realize the rapid flood phase determination and service for every data record; and 2) make sure that the proposed method can be reused and extended. To realize the full life cycle FD&Ss meanwhile ensuring the universality and extensibility, the Process-based FD&S (PFD&S) designed based on sensor web (Broring et al., 2011) was proposed in this paper. The PFD&S method is to provide a way for full life cycle FD&S, and meanwhile ensures the timeliness, universality, and extensibility of the method. It employs ground-based observations as data source, being able to precisely determine the flood phase according to data changes, and to offer customized services to satisfy the varied flood phase - based responding requirements.

In the forthcoming sections, we illustrated the PFD&S method and validated its feasibility for full life cycle FD&Ss. The development of the PFD&S method was presented in Section 2. The overall architecture was described in Section 2.1, the core components illustrated in Section 2.2, and the internal interactions presented in Section 2.3. The design, implementation, and instance of the PFD&S prototype was stated in Section 3, with the prototype design and implementation described in Section 3.1 and 3.2, separately. The experiments and results were provided in Section 4, with the experimental area and data described in Section 4.1, and the sensor provider and event subscriber perspectives elaborated in Section 4.2 and 4.3, respectively. The discussion about the PFD&S method was provided in Section 5, including the accuracy analysis in Section 5.1, comparisons with other FD&S systems in Section 5.2, and limitation statement in Section 5.3. Finally, Section 6 summed up this work and described possible future directions for this study.

2. PFD&S method

Floods occur and develop in the form of process, and determining the flood phases precisely is of great importance to flood monitoring. Different from traditional FD&Ss, the characteristics of the PFD&S method is adopting the idea of process management in the detection and service of floods. To be specific, the main idea of the PFD&S method is to firstly divide the flood process into different phases, then determine the flood phase type based on the filtering of the flood

observations, and finally provide flood services according to the requirements of different flood phases.

2.1. Four-layer architecture

In order to achieve the goal of flood phase detection and service based on flood observations, the data access, the flood phase detection, and the phase-adaptive flood service are mandatory for the PFD&S method. Therefore, as demonstrated in Fig. 1, the PFD&S method consists of the sensor layer, the data access layer, the flood detection layer, and the flood service layer from bottom to top. The sensor layer is to provide the data source, and it is composed of the heterogeneous physical hydrological and meteorological sensors, i.e., water level gauges, etc. The data access layer is responsible for the access of heterogeneous sensors, and it consists of the Access Adapter (AA) (Section 2.2.1) and Sensor Observation Service (SOS) (Broring et al., 2012). The flood detection layer is used to filter the sensor observations and judge on the type of flood phases, and its components include Sensor Event Service (SES) (Echterhoff and Everding, 2008), SOS-SES-Feeder (middleware of SOS and SES), the processing unit, Web Notification Service (WNS) (Simonis and Echterhoff, 2006), and the Process-based Detection Rules (PDR) (Section 2.2.2). The flood service layer mainly to provide customized services according to the type of flood stages, and in this paper, the service types include the Water Level Prediction (WLP) service (Section 3.2), the flood warning service, and the flood statistics service.

The focus of the PFD&S method is on the data access layer, the flood detection layer, and the flood service layer. The overall architecture of the PFD&S method is based on the Open Geospatial Consortium (OGC) information models and service interfaces of Sensor Web (Zhang et al., 2018). The SOS, SES, SOS-SES-Feeder, and WNS used in the PFD&S method are the existing OGC service interfaces. But these services are isolated and cannot be used for FD&S directly. The major contribution of the PFD&S method is to connect and employ these OGC information models and service interfaces to make them universally applicable for the detection and service of flood process. As marked red in Fig. 1, the focus of the PFD&S method is on the AA (Section 2.2.1) of the data access layer, the PDR (Section 2.2.2) and the internal interactions and the processing unit (Section 2.3) of the flood detection layer, and the WLP service (Section 3.2) of the flood service layer.

2.2. Core components

2.2.1. Access adapter

SOS could achieve the sensor access in a standardized way (Broring et al., 2012), but due to the diversity in the flood sensor types and communication protocols, how to transform the diverse flood sensors and observations into the standard forms is still a problem. AA could act as a middleware between physical flood sensors and SOS, and it was proposed for the unified access of heterogeneous flood sensors into SOS. To be specific, AA could be utilized to discover the flood sensors in specific spatiotemporal ranges, remove the abnormalities from the sensor observations, and access the sensors and observations into SOS. As shown in Fig. 2, AA receives sensor metadata from SOS and observation metadata from sensors, and delivers unified observations into SOS. AA is composed of the Data Reception (DR) unit, the Observation Filtering (OF) unit, and the Observation Encoding (OE) unit, and the parameters of all the three units are defined in the configuration file. The DR unit is mainly intended for the acquisition and parse of data streams; the OF unit allows users to perform the observation selection; the OE unit takes the responsibility of unified encoding for observations.

It takes nine steps to use AA to access heterogeneous flood sensors into SOS: (1) Flood sensor metadata is encoded according to Sensor Model Language (SensorML) (Botts and Robin, 2007) and registered into SOS; (2) The DR unit acquires the flood sensor metadata information from the SensorML files; (3) The flood sensor access model is constructed based on the uniform sensor access model template depicted in Fig. 3, and the data stream is organized in accordance with the structure of the data array [SensorID, PropertyID, DataPosition, DataLength, DataRatio]; (4) Data stream is acquired and parsed; (5)–(7) The attribute, temporal, and spatial filtering of the data streams are performed, respectively; (8) The data is encoded according to Observations & Measurements (O&M) (Cox, 2007a, 2007b); and (9) Observations are inserted into SOS. Steps (3)–(4) are completed in the DR unit, steps (5)–(7) in the OF unit, and step (8) in the OE unit. The DR unit has to change with flood sensor types and communication protocols, and the design of separating it from the OF and OE unit could enable AA to work more flexibly and efficiently. The parameters of the DR, OF and OE unit are predefined in the configuration file for flood sensor and data stream access.

2.2.2. Process-based detection rules

PDR is to define a series of rules to determine the flood process, specifically, flood phases. It can be combined with SES to implement the process-based detection of floods. The way of representing flood processes by the four phases of diagnosis, preparedness, response, and recovery is adopted in this paper (Chen et al., 2015). The calculation formula of the PDR is as follows, where formulas (1), (2), (3), and (4) are the conditions needed to be met for each transition between two adjacent flood stages, i.e., diagnosis - preparedness, preparedness - response, response - recovery, and recovery - diagnosis, respectively. Floods are strictly developed in the sequence of diagnosis, preparedness, response, and recovery in the PDR, and satisfying formula (1) indicates flood in the diagnosis stage; meeting both formulas (1) and (2) means flood in the preparedness stage; simultaneously satisfying formula (1), (2) and (3) represents flood in the response phase; meeting formulas (1), (2), (3), and (4) at the same time stands for flood in the recovery phase.

$$\mathrm{Fre}_{T1}(WL < W_1) \geq F_1 \quad (1)$$

$$\mathrm{FreT}_2(W1 \leq WL \leq W2) \geq F2 \quad (2)$$

$$\mathrm{FreT}_3(WL > W2) \geq F3 \quad (3)$$

$$\mathrm{FreT}_4(WL < W3) \geq F4 \quad (4)$$

where WL refers to water level; Fre_{Ti}(Condition i) (i = 1, 2, 3, 4) refers to the occurrence frequency of water level values meeting the condition i in the temporal range of T_i (i = 1, 2, 3, 4); W_1, W_2 and W_3 are the water level thresholds of different flood stages, respectively, satisfying the conditions of $W_1 < W_2$, $W_3 < W_2$; T_1, T_2, T_3, and T_4 are different time window thresholds, and satisfies $T_1 \geq T_2 \geq T_3 \geq T4$; F_1, F_2, F_3 and F_4 are occurrence frequency thresholds of different flood phases. As the safety and warning water level values are determined by analyzing lots of historic flood records and regional environments, and they are of great guiding significance for detecting floods, W_1 and W_2 here equal to the safety and warning water levels, separately, and W_3 usually satisfies the condition of $W_1 < W_3 < W_2$. In PDR, the response phase is essential, and only the flood events with the response phase are the true flood events that will be dealt with or recorded to reduce the error detection rate.

2.3. Internal interactions

The mechanism of information delivery and internal interactions among the layers of the PFD&S method is elaborated in this section. As the sensor layer only acts as the sensor and data provider in the PFD&S method, and it does not have many internal interactions with other layers, therefore, it will not be further elaborated here. The internal interactions of the data access layer, flood detection layer, and the flood service layer in the PFD&S method are demonstrated in Fig. 4.

The internal interactions of the data access layer, flood detection

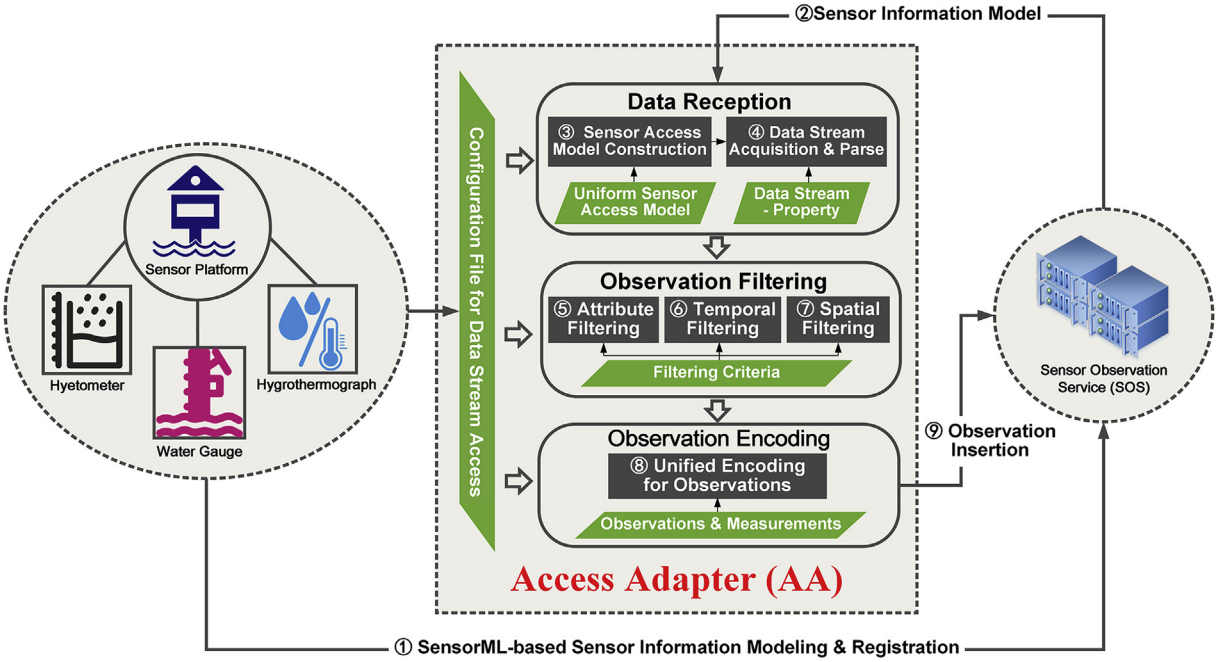

Fig. 2. Main components of AA and its interactions with SOS.

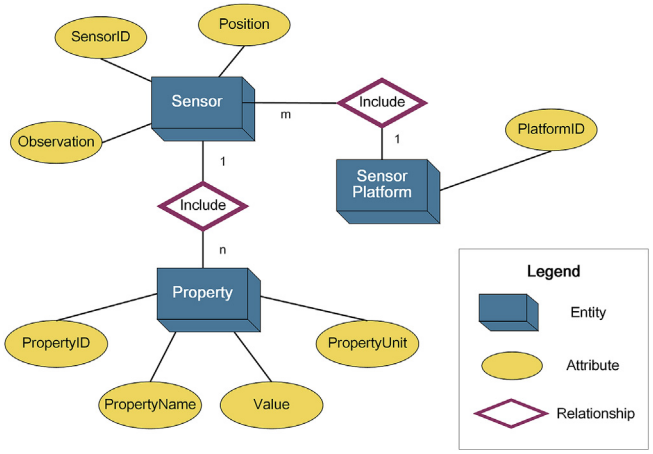

Fig. 3. The uniform sensor access model defined in the DR unit.

layer, and the flood service layer could be interpreted from the two perspectives of flood sensor providers and flood event subscribers. The two perspectives correspond to the flood sensor - oriented and the flood event subscriber - oriented service patterns of the PFD&S method. As for the flood sensor provider - oriented service pattern, the major contribution of the PFD&S method is to provide the mechanism for sensor data publishing and sharing, which can be realized by the following five steps: (1) Heterogeneous sensors are accessed and sensor observations are inserted into SOS by AA via the RegisterSensor and InsertObservation operations, respectively; (2) SOS-SES-Feeder actively sends the DescribeSensor request to SOS and receives the SensorML files from SOS; (3) SOS-SES-Feeder registers the sensor lists to SES through the RegiterPublisher operation and gets the registered publisherID from SES; (4) SOS-SES-Feeder sends the GetObservation request to SOS and receives the O&M files from SOS; (5) SOS-SES-Feeder notifies the sensor observation lists to SES.

After flood sensor providers publish and share their flood monitoring sensors and observations, flood event subscribers could subscribe the floods of their interest by submitting their flood event subscription requests. The flood event subscriptions could be implemented by the following six steps: (1) Flood event subscriber sets the parameters for the PDR (i.e., flood sensor ID, and threshold, etc.) and the WLP service (i.e., maximum error, and iteration, etc.) (Section 3.2); (2) PDR is encoded according to the Event pattern Markup Language (EML) (Everding and Echterhoff, 2008) and the flood event subscription model is formed; (3) The flood event subscription model is submitted to SES; (4) SES performs the data filtering, completes the current flood stage judgment according to the flood event subscription model, and further transmits the current flood event phase information to the processing unit; (5) The processing unit performs the flood stage change detection, and deliver the true flood phase information to WNS; and (6) Corresponding flood service is activated, and the true phase detection result and notifications are returned to the flood event subscriber.

3. PFD&S prototype design and implementation

3.1. Prototype design

A prototype was developed based on the PFD&S method proposed in this paper. The prototype is designed conforming to the OGC sensor web standards, and it is Browser/Server based, with the client and server separated. The PFD&S prototype can be divided into four tiers, including the database tier, the intermediary service tier, the business logic tier, and the user interaction tier. The database tier is composed of the SOS database, the SOS-SES-Feeder database, the subscription management database of SES, and the flood database. The intermediary service tier consists of Apache Storm, SOS, SES, SOS-SES-Feeder, and WNS. The business logic tier is the core tier of the PFD&S prototype, and it is composed of the businesses of the flood event subscription encoding and registration, OGC sensor web standards parsing, login logic judgement, flood phase services, and data access, etc. There are six function modules in the user interaction tier, including the user registration/login, the flood sensor access management, the flood sensor map display, the flood event subscription, the flood event management, and the flood phase service modules.

3.2. Prototype implementation

The whole architecture of the PFD&S prototype was implemented

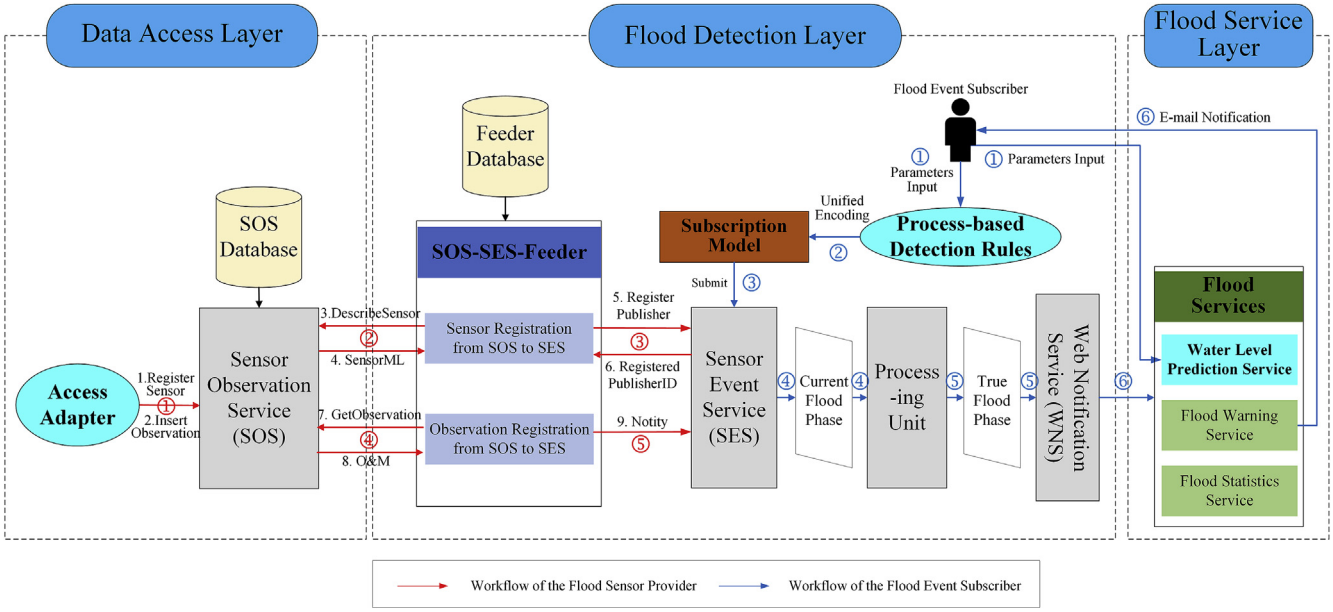

Fig. 4. Internal interactions of the data access layer, flood detection layer, and the flood service layer in the PFD&S method.

based on the open source code of 52°North (52n) (https://52north.org/), because of its supporting more operations and continuously updating. The client adopts the React framework, and utilizes the components of the Ant Design 2.13.11 to implement the basic design, the React-Amap 1.1.3 to complete the map function, and the React-Highcharts 15.0.0 to enrich the data display. The server employs the Spring MVC and Hibernate framework supported by Apache Storm 1.0.0, 52n SOS 3.5.0, 52n SES 1.2.2, 52n SOS-SES-Feeder 1.0.0, and WNS 0.1.0. The database used is PostgreSQL 9.2, which is open source, and features powerful functions in supporting spatial operations. The programming language employed is Java, JavaScript, CSS, and Html.

Improvement was made on the WLP service of the PFD&S prototype, so how to implement it is elaborated here. The WLP service in this paper adopts the Back Propagation Neural Network (BPNN) (Li et al., 2017) method to predict water levels. BPNN has the capability of auto-learning without requiring prior knowledge, the back propagation mechanism of errors, and could realize any nonlinear mapping from input to output with higher accuracy, making it suitable for resolving the problems with complicated internal mechanisms, i.e., WLP (Ghose et al., 2010). Due to the fact that the accuracy of the BPNN results can be affected by many factors except for basin precipitation, this paper makes improvement on the input vectors to improve the prediction accuracy. Instead of just using basin precipitation to make predictions, the WLP service here adopts nine factors, including upstream water level, air pressure, air temperature, ground temperature, wind speed, precipitation, evapotranspiration, relative humidity, and sunlight exposure duration of the watershed as input vectors for downstream water level predicting.

4. Experiments and results

4.1. Experimental area and data

With the total length of 1532 km, the Hanjiang river is the first longest tributary of the Yangtze River (the longest river in China and Asia, and the third longest river worldwide), and it also has the maximum annual variation of runoff among all the tributaries of the Yangtze River. Huanghan basin is one of the sub-basins located in the middle and lower reaches of the Hanjiang basin. With the riverbed slope becoming smaller and the water flow turning slow, floodings frequently occur in the Huanghan basin. The area of the Huanghan basin is $5.04 \times 10^4\,km^2$, with the terrain of the basin high in the northwest while low in the southeast, and the geology is mainly composed of middle or low mountains in the northwest while dominated by plains or hills in the southeast. Located in the subtropical monsoon region, the Huanghan basin has the mild and humid climate and an ample annual precipitation of 700–1000 mm (Chen et al., 2007). However, the rainfall distribution is spatial-temporally uneven, with the precipitation gradually increasing from the upper to the lower basin, and the runoff from May to October accounting for about 75% of the whole year. Therefore, it is of great significance to perform flood detecting research in the Huanghan basin.

As shown in Fig. 5, there are eight hydrological stations, i.e., Huangjiagang, Xiangyang, Huangzhuang, Shayang, Yuekou, Xiantao, and DiaochaLake, in the upstream, and Hanchuan station downstream, and five meteorological stations, i.e., Fangxian, Gucheng, Zhongxiang, Tianmen, and Xiaogan, evenly distributed in the Huanghan basin. Two flood events occurred in the experimental area in July 2016 were taken as examples to verify the feasibility and validation of the PFD&S method. The annual changes of precipitations in the Xiaogan station, the nearest meteorological station to the Hanchuan hydrological station, and those of water levels in the Hanchuan station in 2016 are shown in Fig. 6.

The water levels of Hanchuan station were used in the full life cycle flood detecting. The seven upstream hydrological observation stations, i.e., Huangjiagang, Xiangyang, Huangzhuang, Shayang, Yuekou, Xiantao, and DiaochaLake, and five evenly distributed meteorological stations, i.e., Fangxian, Gucheng, Zhongxiang, Tianmen and Xiaogan, were employed in predicting the water levels of Hanchuan Station. Among them, the monitoring variable of the hydrological stations is water level, and the monitoring variables of the meteorological stations are eight kinds of meteorological factors, including air pressure, air temperature, land surface temperature, wind speed, precipitation, evapotranspiration, relative humidity and sunlight exposure duration. The data used in the experiment ranged from January 1, 2000 to December 31, 2016, and the data sampling frequency was once per day. In the experiment, the flood simulation began from July 1, 2016, and to facilitate the simulation of the historic floods, the sampling frequency of the experimental data was all set to once per minute. Therefore, the observation at the nth minute from the beginning of the experiment corresponded to that at the nth day from July 1, 2016.

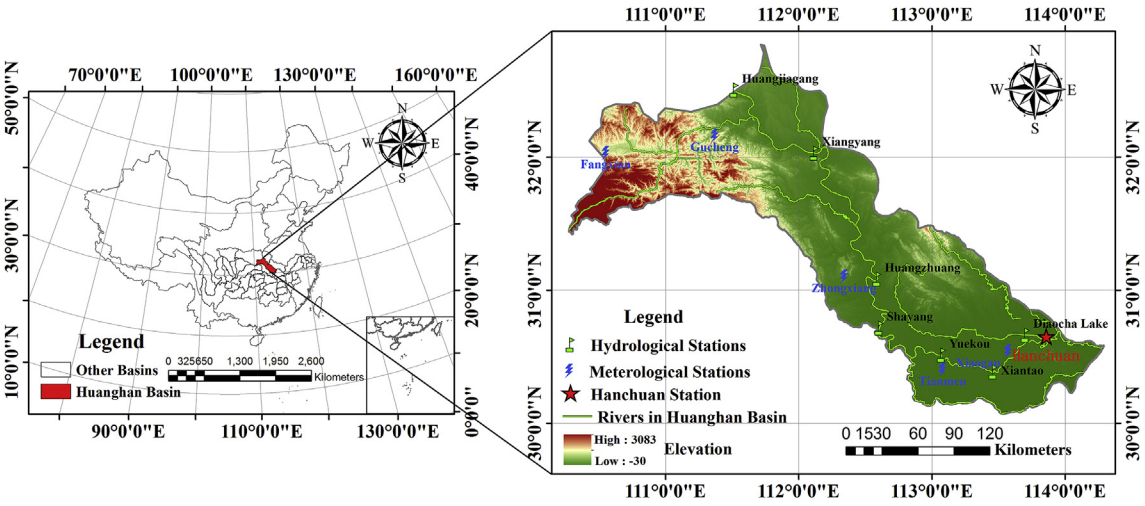

Fig. 5. Experimental area (the Huanghan basin) and the distribution of hydrological and meteorological stations.

4.2. Sensor provider perspective

Sensor providers could utilize the data access function of the PFD&S prototype to publish and share their sensor observations. The data access interface of the PFD&S prototype is shown in Fig. 7. Sensor providers could complete the data access by firstly encoding the sensor information according to SensorML, secondly defining the parameters of the data array in the data access layer, and finally uploading the configuration file for access. In this paper, the configuration files of the eight hydrological stations, i.e., Hanchuan, Huangjiagang, Xiangyang, Huangzhuang, Shayang, Yuekou, Xiantao, and DiaochaLake, and the five meteorological stations, i.e., Fangxian, Gucheng, Zhongxiang, Tianmen and Xiaogan, were all uploaded for use. The communication protocols of all these sensors include Modbus and XPH. After sensor providers accessed these sensors into the PFD&S prototype, event subscribers could select and activate the sensors they needed for further processing.

4.3. Event subscriber perspective

From the perspective of event subscribers, after submitting flood event subscription to the PFD&S prototype, they could acquire the detection results and receive messages from the corresponding flood services.

4.3.1. Event subscription

To complete the flood event subscription, there are three operations requiring interactions with flood event subscribers, including the sensor selection and the parameter setting of PDR and the WLP service. The sensor selection interface of the PFD&S prototype is shown in Fig. 8, with all the sensors accessed listed. The sensor(s) selected here would be utilized in PDR for full life cycle flood detecting. “Hanchuan Station” was selected in the experiment to provide the data source for detecting the floods occurring in the Huanghan basin.

After the user completed the sensor selection, they were required to input the threshold, time window, repeated times, and other parameters required in PDR. The parameter setting interface of PDR in the PFD&S prototype was shown in Fig. 9, and the system would automatically generate the subscription model when received the parameters. The water level thresholds $W_1 = 28$, $W_2 = 29$, and $W_3 = 28.5$ were used in the mitigation, preparedness, response, and recovery phases of PDR in this experiment. $W_1 = 28$ and $W_2 = 29$ were the

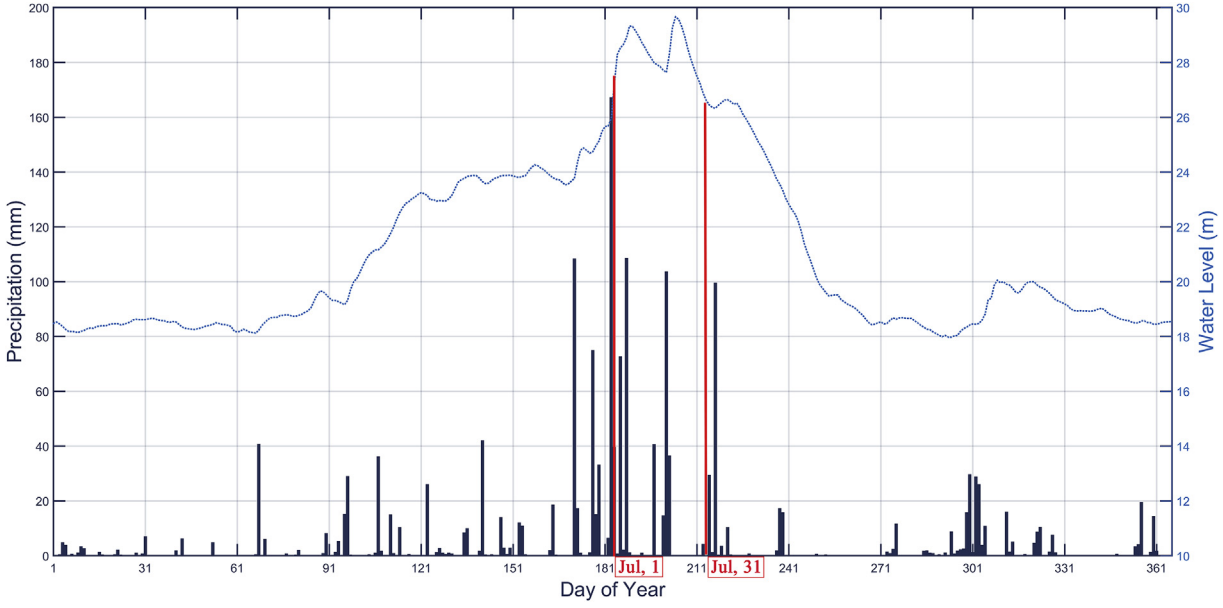

Fig. 6. Annual precipitation changes of the Xiaogan meteorological station and Annual water level changes of the Hanchuan hydrological station in 2016.

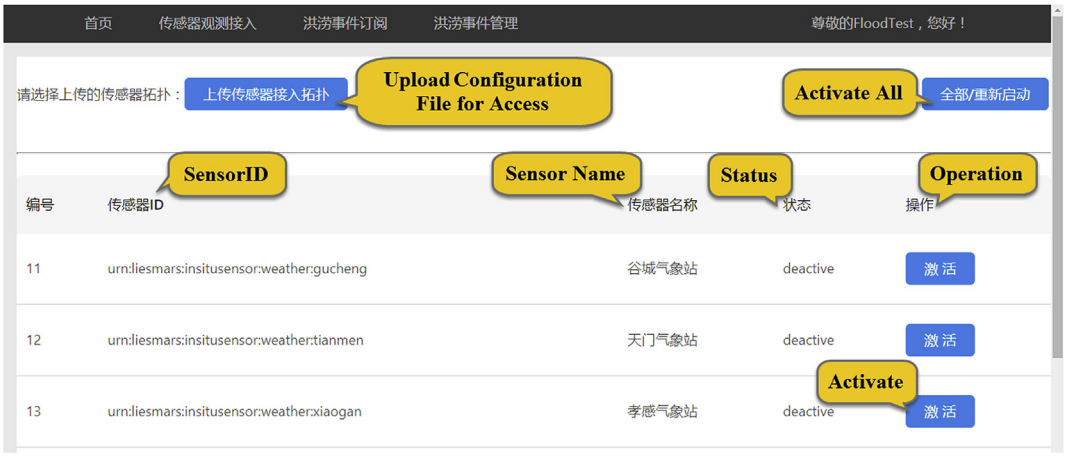

Fig. 7. The sensor access interface of the PFD&S prototype.

guaranteeing and warning water levels of the Hanchuan hydrological observation station issued by the Hubei Provincial Department of Water Resources, respectively, and $W_3 = 28.5$ was determined by trial and error. The time windows and occurrence frequency thresholds of all the four phases, are one second, and once, respectively.

Fig. 10 shows the parameter configuration interface of the WLP service. The parameters required to be set include the learning rate, the maximum iterations, the maximum error, and the hydrological or meteorological stations and their observed properties involved. The water level of the seven hydrological stations, i.e., Huangjiagang, Xiangyang, Huangzhuang, Shayang, Yuekou, Xiantao, and DiaochaLake, and the eight types of observed properties, i.e., air pressure, air temperature, land surface temperature, wind speed, precipitation, evapotranspiration, relative humidity, and sunlight exposure duration, of the five meteorological stations, i.e., Fangxian, Gucheng, Zhongxiang, Tianmen, and Xiaogan were all selected as the input of the WLP service in this experiment.

This experiment used the hydrological and meteorological data of the Huanghan basin from 2000 to 2015 as the training data to construct the BPNN, and the data in 2016 as the test data. Specifically, the observations in the continuous 100 time instants were used as input and the water levels on the 101st and 102nd time instants were used as output. The network structure of the WLP service was set as (47, 4, 7, 1) through trial and error, with 47 and 1 the dimensions of the input and output vector, separately, and 4 and 7 determined by keeping the other unchanged meanwhile lowering the error into minimum. The learning rate was set to 0.01 via the mesh filter method, the maximum error set to 1.0×10^{-8}, and the maximum number of iterations set to 5.0×10^{4} times. In addition, the E-mail receiving address of the flood event notification message and the alias of the flood event were also set in this module. The parameter summary of PDR and the WLP service was shown in Fig. 11.

4.3.2. Detection results

Once receiving the parameters set for PDR, the PFD&S prototype automatically transformed them into the flood event subscription model. Based on the subscription model, SES filtered the data streams of the sensor selected and determined the current flood phase. Then the

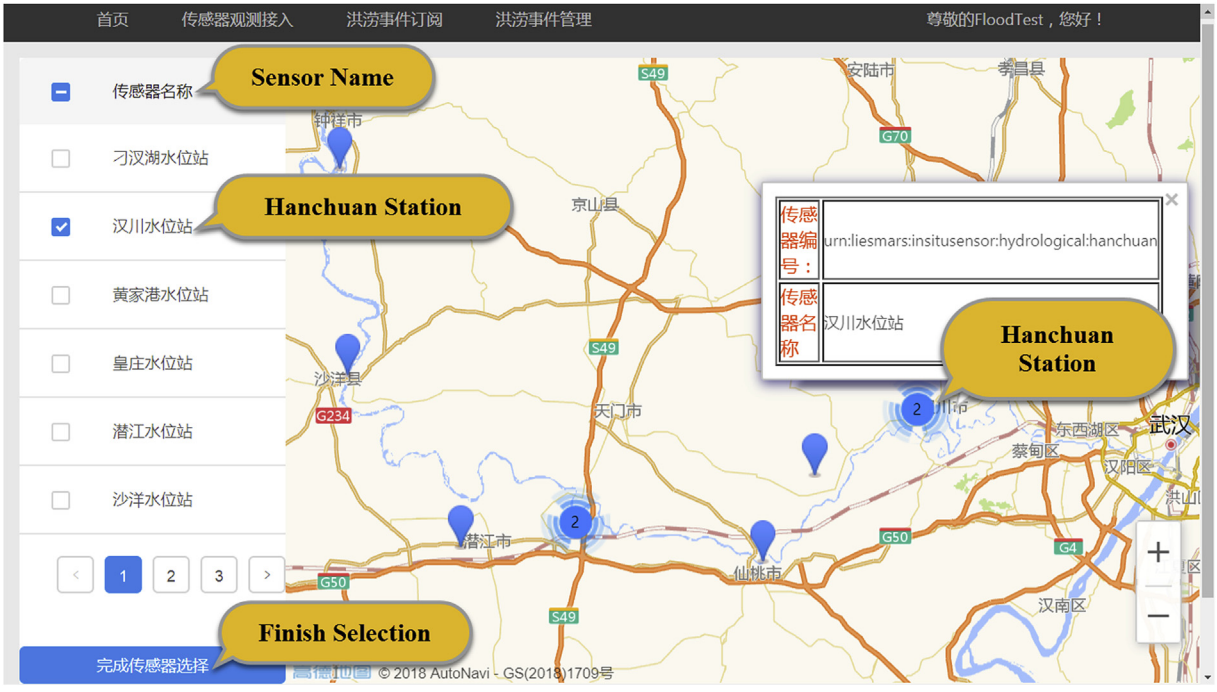

Fig. 8. Sensor selection interface of the PFD&S prototype.

Fig. 9. Parameter setting interface of PDR in the PFD&S prototype.

processing unit compared the current flood phase with those of the previous time instants, and made judgment on the true flood phase. The PFD&S method could realize the flood phase judgement for each data item, thus here it could determine the flood phase for each minute. The detection result of flood process was demonstrated in Fig. 12.

As the historic flood events were simulated as real-time in the experiment, there exists a correspondence between the experimental time and the actual time. The mapping from the experimental time to the actual time was displayed in Table 1. The flood simulation experiment began at 13:28 on April 12, 2018, and it corresponded to the actual time of July 1, 2016. Every minute in the experiment was equivalent to one day of the actual time, therefore, 13:29, 13:33, 13:39, 13:41, 13:45, 13:46, 13:47, 13:53, and 13:54 representing July 2, July 6, July 12, July 14, July 18, July 19, July 20, July 26, and July 27 of 2016, respectively.

As can be seen from Table 1, there were two complete flood events from July 1 to July 30, 2016. The first flood event lasted from July 1 to July 14, 2016, in which it began on July 1, entered the preparedness phase on July 2, further went into the response phase on July 6, then was back to the recovery phase on July 12, and finally ended on July 14 in 2016. The second flood event lasted from July 18 to July 27, in which it began on July 18, entered the preparedness phase on July 19, further went into the response phase on July 20, then was back to the recovery phase on July 26, and finally ended on July 27 in 2016.

4.3.3. *Flood services*

There were three types of flood services in the PFD&S prototype, including the WLP, the flood warning and the flood statistics services. The WLP service was utilized in all the four flood phases of diagnosis, preparedness, response, and recovery. The flood warning service was adopted in both the preparedness and response phases. The flood statistics service was only employed in the discovery phase.

4.3.3.1. WLP service. The WLP service of the PFD&S prototype was realized based on BPNN, and it could predict the water levels in the future 48 time instants. By providing users with future trends of water level changes, the WLP service can be combined with PDR to enable users to make timely decisions and responses. The WLP service worked

Fig. 10. Parameter configuration interface of the WLP service.

Fig. 11. Parameter summary interface of PDR and the WLP service.

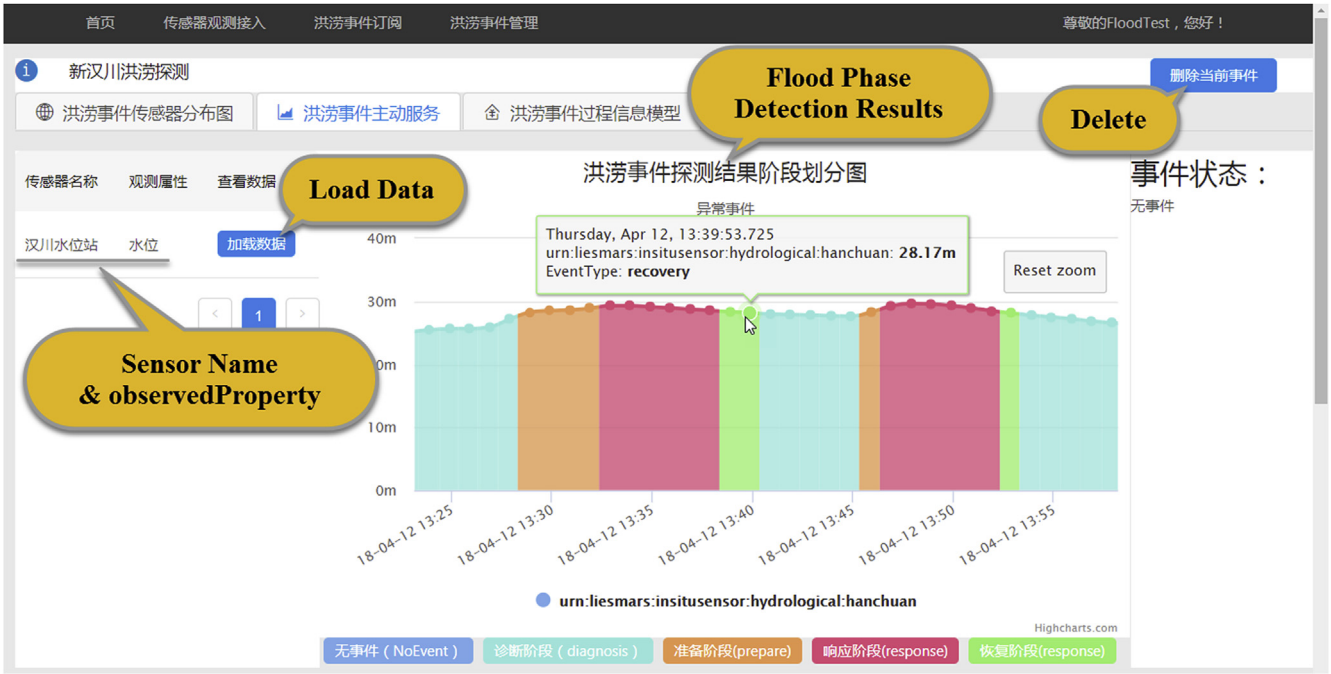

Fig. 12. Demonstration interface of the flood process detection result in the PFD&S prototype.

through the whole process of floods, and Fig. 13 showed the record interface of the WLP service in the PFD&S prototype. The prediction result chart on the right side of Fig. 13 displayed the WLP results in 102 time instants, of which 100 time instants were before the prediction time and 2 time instants afterwards. According to the mapping rule of time, the first record in the middle of Fig. 13 demonstrated that the Huanghan basin flood event was in the preparedness phase on July 3, 2016, and the predicted water level on July 4 and 5, 2016 were 28.41 and 28.42 m, respectively, indicating that the water level would continue to rise in the near future.

4.3.3.2. Flood alert service. The purpose of the flood alert service is to clearly inform the user of the current flood phase and the WLP results in the future two time instants of the flood events they subscribed. Once floods entered the preparedness or response phase, the PFD&S prototype would send a flood warning notification to the user by E-mail. Fig. 14(a) shows the management interface of the flood alert messages in the PFD&S prototype. Fig. 14(b) corresponded to the third

Table 1
The mapping of the flood phase detection results from the experimental time to the actual time. B refers to the beginning time, and E represents the ending time.

Phase B/E	1st Flood		2nd Flood	
	Experimental Time	Actual Time	Experimental Time	Actual Time
Diagnosis (B)	13:28 April 12, 2018	July 1, 2016	13:45 April 12, 2018	July 18, 2016
Preparedness (B)	13:29 April 12, 2018	July 2, 2016	13:46 April 12, 2018	July 19, 2016
Respond (B)	13:33 April 12, 2018	July 6, 2016	13:47 April 12, 2018	July 20, 2016
Recovery (B)	13:39 April 12, 2018	July 12, 2016	13:53 April 12, 2018	July 26, 2016
Recovery (E)	13:41 April 12, 2018	July 14, 2016	13:54 April 12, 2018	July 27, 2016

flood alert record in Fig. 14(a), and demonstrated the content of the flood alert E-mail sent by the PFD&S prototype. It informed users of that the Huanghan basin flood event he/she subscribed had entered the response stage on July 6, 2016, and the water levels on July 7 and 8, 2016 would be 29.17 and 29.03 m, respectively. The predicted results indicated that the water levels would decrease slowly, and the flood would be relieved soon.

4.3.3.3. Flood statistics service. Flood statistics service is to complete the information archiving and management of flood events according to the four stages of diagnosis, preparedness, response, and recovery. After the flood event was completely over, the PFD&S prototype would invoke the flood statistics service to make statistics on the information of the whole flood process, including the maximum water level values, and the beginning and ending time of different stages, etc. Fig. 15 showed the two complete flood statistics records of this experiment. The right side of Fig. 15 displayed the details of the second flood event statistics record, indicating that the event began on July 18, entered the preparedness phase on July 19, further went into the response phase on July 20, and on the same day the water level reached the maximum of 29.66 m, then was back to the recovery phase on July 26, and finally ended on July 27 in 2016.

5. Discussion

5.1. Accuracy analysis

5.1.1. Detection accuracy

The PFD&S detection results were compared with the authoritative flood record to achieve the evaluation of the detection accuracy. As displayed in Table 2, the comparison results demonstrated that in the experiment, the PFD&S method could accurately detect the beginning time of the response phase of the flood events without no delay or advance. Moreover, the PFD&S method is able to detect the entering time of the preparedness time of the flood events 1 or 4 days ahead, proving that the PFD&S method proposed in this paper possessed the capability of early detection and high detection accuracy. At the same time, the detection results could elaborately divide the flood process into diagnosis, preparedness, response and recovery phases, more accurately characterizing the floods and providing solid foundations for the subsequent statistics and analysis.

5.1.2. Prediction accuracy

To evaluate the prediction accuracy of the WLP service, the prediction results of the WLP service adopting multiple meteorological data were compared with those derived only from the precipitation data, and the ground truth. The accuracy analysis of the water level values acquired from the three different methods during the periods of the 1st and 2nd flood was displayed in Table 3. For the 1st flood lasting from July 1, 2016 to July 14, 2016, the Mean Absolute Error (MAE), Mean Relative Error (MRE), and Root Mean Square Error (RMSE) of the WLP service and the only precipitation - based model are 0.67 m and 1.02 m, 2.35% and 3.59%, 0.9942 and 2.1081, separately. For the 2nd flood lasting from July 18, 2016 to July 27, 2016, the MAE, MRE, and RMSE of the MWLP model and the only precipitation - based model are 0.52 m and 0.56 m, 1.81% and 1.95%, 0.6439 and 0.7345, respectively. From the abovementioned statistics analysis, it was proved that by taking the meteorological factors into consideration, the WLP service results were significantly improved when compared with those only

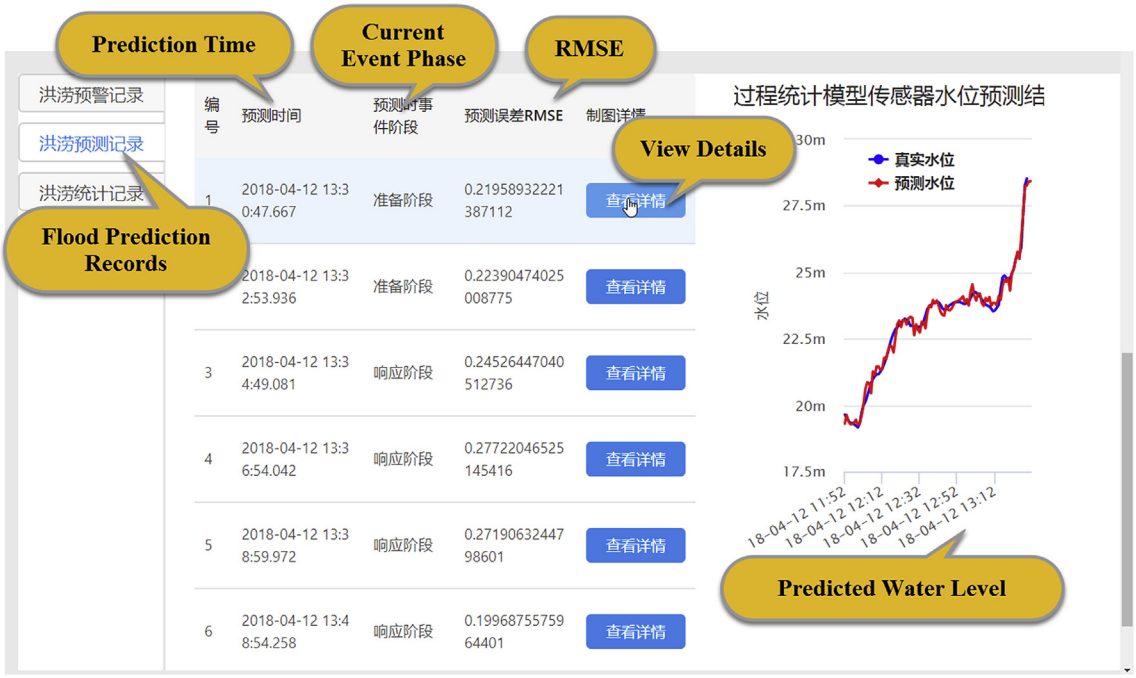

Fig. 13. The record interface of the WLP service in the PFD&S prototype.

Fig. 14. The flood alert record interface and alert E-mail of the PFD&S prototype. (a) The flood alert records interface; (b) The flood alert E-mail.

using the precipitation data and had quite high prediction accuracy.

5.2. FD&S system comparisons

The PFD&S prototype developed in this paper was compared with the existing FD&S systems, i.e., GFDS (Revillaromero et al., 2014), EFAS (Arnal et al., 2018), GloFAS (Alfieri et al., 2013), and DFO (Reager and Famiglietti, 2009), from the perspectives of flood monitoring, notification to users, statistics, forecast, universal data encoding and access, user subscription support, processness, service extensibility, and service instantaneity. The comparison results were shown in Table 4.

5.2.1. Universality

The PFD&S prototype developed in this paper was implemented in accordance with the information models and service interfaces of OGC sensor web (Broring et al., 2011), which enables the unified sharing, processing, and serving of sensor resources. The overall architecture of the PFD&S prototype is universal for both sensor providers and event subscribers of floods. Sensor providers could realize their sensor and observation resource publishing and sharing by conforming to the unified information encoding and data access operations. And event subscribers could subscribe their requests and acquire the flood event information of their interest through supplementing the information of

Table 2
Comparisons between the PFD&S results and the authoritative records. B refers to the beginning time.

Flood	PFD&S Detection Results		Authoritative Records	Accuracy
	Preparedness (B)	Response(B)	Response (B)	
1st Flood	July 2, 2016	July 6, 2016	July 6, 2016	4 days ahead
2nd Flood	July 19, 2016	July 20, 2016	July 20, 2016	1 days ahead

Fig. 15. The flood statistics record interface of the PFD&S prototype.

Table 3
Accuracy analysis of the WLP results. RE refers to relative error.

Flood	Ground Truth	MWLP (Multiple Data – Based)			Only Precipitation Data - Based		
		Predictions	RE	RMSE	Predictions	RE	RMSE
1st Flood	28.29	26.5627	−6.1%	0.9942	20.8513	−26.2%	2.1081
	28.53	25.7770	−9.6%		27. 1784	−4.7%	
	28.66	28.4933	−0.5%		28.4071	−0.8%	
	28.9	28.5016	−1%		28.5143	−1.3%	
	29.33	28.5609	−2%		28.8087	−1.7%	
	29.3	28.7586	−1.8%		28.8467	−1.5%	
	29.14	29.2739	0.4%		28.6212	−1.7%	
	28.96	29.1133	0.5%		28.6513	−1%	
	28.73	28.0094	−2.5%		28.7712	0.1%	
	28.55	27.6364	−3.2%		28.8161	0.9%	
	28.34	28.3188	−0.7%		27.9965	1.2%	
	28.17	27.3037	−3.1%		27.8502	1.1%	
	27.99	27.9940	0.01%		26.0707	−6.86%	
	27.92	28.15891	0.86%		27.7539	−0.60%	
2nd Flood	28.31	27.5451	−2.7%	0.6439	26.7941	−5.3%	0.7345
	29.28	28.3193	−3.2%		28.2704	−3.4%	
	29.66	28.4961	−3.9%		29.1540	−1.7%	
	29.57	29.4164	−0.5%		29.6409	0.2%	
	29.31	29.3274	0.06%		29.6059	1%	
	28.95	29.2183	0.9%		29.5429	2%	
	28.5	29.3541	3%		29.3774	3%	
	28.12	28.3831	0.9%		28.7444	2.2%	
	27.8	28.40534	2.18%		27.5379	−0.94%	
	27.49	27.34155	−0.54%		27.8766	1.41%	

Table 4
Comparisons among different FD&S systems.

Features	PFD&S	GFDS	EFAS	GloFAS	DFO
Flood Monitoring	✓	✓	✓	✓	✓
Flood Notification	✓	×	✓	×	×
Flood Statistics	✓	✓	×	×	✓
Flood Forecast	✓	×	✓	✓	×
Universal Data Encoding & Access	✓	×	×	×	×
User Subscription Support	✓	×	×	×	×
Processness	✓	×	×	×	×
Service Extensibility	✓	×	×	×	×
Instantaneity	2.7 Minutes	Daily	Daily	Daily	Daily

the event subscription template defined inside the prototype. Compared with other systems communicating with specialized standards, the PFD &S system designed based on the universal standards has better universality.

5.2.2. Instantaneity

Three types of time lags exist in this system, i.e., the time lag when transforming the data streams into message flows (named TL_1), the time delay caused by flood phase judgment (named TL_2), and the responding time lag of each service unit (named TL_3). Tl_1 was usually produced during the process of SOS-SES-Feeder firstly pulling flood sensor observations from SOS and then registering them into SES at a specified time interval. TL_2 was often generated in the procedure of processing the messages and detecting the flood phase changes. TL_3 was often caused by the calculation and treatment steps defined in the algorithms of the flood alert (TL_3(1)), prediction (TL_3(2)), or statistics services (TL_3(3)). TL_1, TL_2, TL_3(1), TL_3(2), and TL_3(3) averages to, respectively, 24.6, 92.6, 0.8, 42.2, and 1.2 s, after the experiment was repeated 10 times under the same computation environment. As the three steps of data stream transformation, flood phase judging, and WLP are mandatory for flood detection, the time delay of acquiring the detection results is the sum of TL_1, TL_2, and TL_3(2). That is, the PFD &S system could achieve the flood detection in 159.4 s, with high instantaneity and demonstrating great superiority over other FD&S systems, i.e., GFDS, EFAS, GloFAS, and DFO, updating at a daily basis.

5.2.3. Extensibility

To access more sensors, serve more flood detections, and satisfy more diverse flood service requests, the PFD&S prototype was designed to be extensible. The extensibility of the PFD&S prototype lies in the three following aspects: the sensor types and numbers, the flood detection models, and the flood service types. The extensibility of sensor types and numbers is reflected in the flexibility of the data access layer of the PFD&S prototype, due to AA which separates the data reception unit from the data filtering and encoding unit, new types of sensors could be accessed easily by modifying the configuration file. If event subscribers want to utilize other flood detection models instead of the PDR proposed in this paper for flood detection, what they are only required to do is encapsulating their new flood detection model according to the patterns of EML and applying them in SES. As for flood services, the IPhaseService interface was predefined in the PFD&S prototype, and new types of flood phase services could be added by implementing the executeService() method of the interface and modifying the configuration file for the type announcement of flood phase services, correspondingly.

5.2.4. Processness

As for processness, instead of only detecting whether flood events would occur or not coarsely as the existing FD&S methods and systems, the PFD&S method and prototype proposed in this paper could precisely determine the flood phase according to each item of flood sensor observations. This flood process detection is able to help in intuitively embodying the whole occurrence and development process of floods, making it more efficiently and conveniently for flood preparedness and responding.

5.3. Limitations

Although featuring great universality, instantaneity, extensibility, and processness, the PFD&S method and prototype also has its own weaknesses. Firstly, the four phases defined in PDR occurred sequentially, so flash floods which occur in the time period shorter than the data sampling intervals will not be correctly detected. But this problem can be resolved by higher data sampling rate. Secondly, this paper only

utilized PDR to provide a useful exploration for flood process detection, and more elaborated models should be proposed and applied in flood detecting. Additionally, only three types of flood services were provided in the PFD&S prototype, not enough for diverse service requirements from water authorities and citizens, and more service types, i.e., route planning, and supply allocation, etc., should be further added.

6. Conclusion and outlook

As for the rapid and continuous flood detection for regions without adequate data support, there are mainly two problems faced with them, including how to rapidly implement the full life cycle flood detecting, and how to further ensure the universality and extensibility of the flood detection method. To solve the abovementioned two problems, this paper proposed the PFD&S method by combining PDR with sensor web, and designed and implemented the PFD&S prototype. To validate the PFD&S method and prototype, the Huanghan basin (Hubei, China) was selected as the experimental area, and the two flood events occurring in July 2016 was selected as flood examples.

Two floods were detected in the experiment, and the flood phases of them were accurately divided, with the process of the 1st and 2nd floods being July 1 - July 2 - July 6 - July 12 - July 14, and July 18 - July 19 - July 20 - July 26 - July 27 in 2016, respectively. Compared with the authoritative flood records, the 1st and 2nd flood were detected to enter the preparedness phase four and one days in advance, respectively, and the detected beginning time of the response phase of the two floods were totally accurate without delay or advance. In addition, the MAE, MRE, and RMSE of the WLP service for the 1st and 2nd flood was 0.67 m, 2.35%, 0.9942, and 0.52 m, 1.81%, and 0.6439, separately, and the corresponding jobs of flood alert e-mail sending and flood information statistics were also completed. In addition, the whole flood process detection and service of the PFD&S method could be finished instantly in 2.7 min. Moreover, the PFD&S prototype features great universality, extensibility, and processness when it was in comparison with other FD&S prototypes, i.e., GFDS, EFAS, GloFAS, and DFO. In summary, the PFD&S method proposed in this paper was proved to have fulfilled its design objective of rapid full life cycle flood detection while possessing the capability of universality and extensibility. But flood service types provided by the PFD&S prototype were limited, more flood service types need to be expanded in future researches to meet more diversified flood management requirements.

Acknowledgements

This work was supported by grants from the China Postdoctoral Science Foundation (No. 2017M622502), the National Key R&D Program of China (No. 2017YFB0503800), the National Natural Science Foundation of China (no. 41601406, 41771422), the Natural Science Foundation of Hubei Province, China (no. ZRMS2017000698), the CRSRI Open Research Program, China (No. CKWV2018487/KY), and the LIESMARS Special Research Funding, China. We thank the National Meteorological Science Data Sharing Service Platform of China for the free download of the meteorological data.

Appendix

Acronyms used in this paper was listed in Table A.1.

Table A.1
Acronyms used in this paper.

Acronyms	Complete Expressions
FD&S	Flood Detection and Service
PFD&S	Process - based Flood Detection and Service
IAB	Inundated Area - Based
SDB	Submerged Depth - Based
DOVB	Direct Observation Variables - Based
GFDS	Global Flood Detection System
EFAS	European Flood Alert System
GloFAS	Global Flood Awareness System
DFO	Dartmouth Flood Observatory
OGC	Open Geospatial Consortium
AA	Access Adapter
SOS	Sensor Observation Service
SensorML	Sensor Model Language
O&M	Observations and Measurements
SES	Sensor Event Service
WNS	Web Notification Service
PDR	Process - based Detection Rules
WLP	Water Level Prediction
DR	Data Reception
OF	Observation Filtering
OE	Observation Encoding
BPNN	Back Propagation Neural Network
EML	Event pattern Markup Language
MAE	Mean Absolute Error
MRE	Mean Relative Error
RMSE	Root Mean Square Error

Appendix A. Supplementary data

Supplementary data to this article can be found online at https://doi.org/10.1016/j.envsoft.2019.03.004.

References

Acosta-Coll, M., Ballester-Merelo, F., Martínez-Peiró, M., 2018. Early warning system for detection of urban pluvial flooding hazard levels in an ungauged basin. Nat. Hazards 92 (4), 1–29.

Amitrano, D., Martino, G.D., Iodice, A., Riccio, D., Ruello, G., 2018. Unsupervised rapid flood mapping using Sentinel-1 GRD SAR images. IEEE T. Geosci. Remote 99, 1–10.

Alfieri, L., Burek, P., Dutra, E., Krzeminski, B., Muraro, D., Thielen, J., Pappenberger, F., 2013. GloFAS – global ensemble streamflow forecasting and flood early warning. Hydrol. Earth Syst. Sci. 17 (3), 1161–1175.

Arnal, L., Cloke, H.L., Stephens, E., Wetterhall, F., Prudhomme, C., Neumann, J., Krzeminski, B., Pappenberger, F., 2018. Skilful seasonal forecasts of streamflow over Europe? Hydrol. Earth Syst. Sci. Discuss. 22 (4), 1–27.

Auynirundronkool, K., Chen, N., Peng, C., Yang, C., Gong, J., Silapathong, C., 2012. Flood detection and mapping of the Thailand central plain using Radarsat and MODIS under a sensor web environment. Int. J. Appl. Earth Obs. 14 (1), 245–255.

Botts, M., Robin, A., 2007. OpenGIS® Sensor Model Language (SensorML) Implementation Specification (Version: 1.0). OGC Document Number: 07-000. Open Geospatial Consortium, Wayland, MA, USA.

Broring, A., Echterhoff, J., Jirka, S., Simonis, I., Everding, T., Stasch, C., Liang, S., Lemmens, R., 2011. New generation sensor web enablement. Sensors 11, 2652–2699.

Broring, A., Stasch, C., Echterhoff, J., 2012. OGC Sensor Observation Service Interface Standard (Version: 2.0). OGC Document Number: 12-006. Open Geospatial Consortium, Wayland, MA, USA.

Cane, D., Ghigo, S., Rabuffetti, D., Milelli, M., 2013. Real-time flood forecasting coupling different postprocessing techniques of precipitation forecast ensembles with a distributed hydrological model. The case study of May 2008 flood in western Piemonte, Italy. Nat. Hazard Earth Sys 13 (2), 211–220.

Caruso, B.S., Rademaker, M., Balme, A., Cochrane, T.A., 2013. Flood modelling in a high country mountain catchment, New Zealand: comparing statistical and deterministic model estimates for ecological flows. Int. Assoc. Sci. Hydrol. Bull. 58 (2), 328–341.

Chen, H., Guo, S., Xu, C.Y., Singh, V.P., 2007. Historical temporal trends of hydro-climatic variables and runoff response to climate variability and their relevance in water resource management in the hanjiang basin. J. Hydrol. 344 (3–4), 171–184.

Chen, N.C., Du, W., Song, F., Chen, Z.Q., 2015. FLCNDEMF: an event metamodel for flood process information management under the sensor web environment. Rem. Sens. 7 (6), 7231–7256.

Cian, F., Marconcini, M., Ceccato, P., 2018. Normalized difference flood index for rapid flood mapping: taking advantage of EO big data. Remote Sens. Environ. 209, 712–730.

Cohen, J., Riihimäki, H., Pulliainen, J., Lemmetyinen, J., Heilimo, J., 2016. Implications of boreal forest stand characteristics for X-band SAR flood mapping accuracy. Remote Sens. Environ. 186, 47–63.

Cox, S., 2007a. Observations and Measurements - Part 1 - Observation Schema (Version: 1.0). OGC Document Number: 07-022r1. Open Geospatial Consortium, Wayland, MA, USA.

Cox, S., 2007b. Observations and Measurements – Part 2 - Sampling Features (Version: 1.0). OGC Document Number: 07-002r3. Open Geospatial Consortium, Wayland, MA, USA.

Dai, Y., Trigg, M.A., Ikeshima, D., 2015. Development of a global ~ 90 m water body map using multi-temporal landsat images. Remote Sens. Environ. 171, 337–351.

Darand, M., Sohrabi, M.M., 2018. Identifying drought- and flood-prone areas based on significant changes in daily precipitation over Iran. Nat. Hazards 90 (3), 1427–1446.

Demir, I., Krajewski, W.F., 2013. Towards an integrated flood information system: centralized data access, analysis, and visualization. Environ. Model. Softw 50 (4), 77–84.

Du, W., Chen, N., Liu, D., 2017a. Automatic balloon snake method for topology adaptive water boundary extraction: using GF-1 satellite imagery as an example. IEEE J. Sel. Top. Appl. Earth Observ. Remote Sens. 99, 1–14.

Du, W., Chen, N., Liu, D., 2017b. Topology adaptive water boundary extraction based on a modified balloon snake: using GF-1 satellite images as an example. Rem. Sens. 9 (2), 140.

Echterhoff, J., Everding, T., 2008. OpenGIS® Sensor Event Service Interface Specification (Proposed) (Version: 0.3.0). OGC Document Number: 08-133. Open Geospatial Consortium, Wayland, MA, USA.

Everding, T., Echterhoff, J., 2008. Event Pattern Markup Language (EML) (Version: 0.3.0). OGC Document Number: 08-132. Open Geospatial Consortium, Wayland, MA, USA.

Feng, Y., Sester, M., 2018. Extraction of pluvial flood relevant volunteered geographic information (VGI) by deep learning from user generated texts and photos. ISPRS Int. J. Geo-Inf. 7 (2), 39.

Fohringer, J., Dransch, D., Kreibich, H., Schröter, K., 2015. Social media as an information source for rapid flood inundation mapping. Nat. Hazard Earth Sys. 3 (3), 4231–4264.

Gao, W., Shen, Q., Zhou, Y., Li, X., 2018. Analysis of flood inundation in ungauged basins based on multi-source remote sensing data. Environ. Monit. Assess. 190 (3), 129.

Ghose, D.K., Panda, S.S., Swain, P.C., 2010. Prediction of water table depth in western region, Orissa using BPNN and RBFN neural networks. J. Hydrol. 394 (3–4), 296–304.

Giordan, D., Notti, D., Villa, A., Zucca, F., Calò, F., Pepe, A., Dutto, F., Pari, P., Baldo, M., Allasia, P., 2018. Low cost, multiscale and multi-sensor application for flooded areas mapping. Nat. Hazard Earth Sys. 18 (5), 1493–1516.

Guha-Sapir, D., Hoyois, Ph, Below, R., 2016. Annual disaster statistical review 2016: the numbers and trends. Available: http://www.cred.be/sites/default/files/ADSR_2016.pdf, Accessed date: 6 April 2018 Access on.

Hirsch, R.M., Archfield, S.A., 2015. Flood trends: not higher but more often. Nat. Clim. Change 5 (3), 198.

Jongman, B., Wagemaker, J., Romero, B., De Perez, E., 2015. Early flood detection for rapid humanitarian response: harnessing near real-time satellite and twitter signals. ISPRS Int. J. Geo-Inf. 4 (4), 2246–2266.

Li, S., Xu, Y., He, Y., Geng, Z., Jiang, Z., Zhu, Q., 2017. Research on public opinion warning based on analytic hierarchy process integrated back propagation neural network. In: 2017 Chinese Automation Congress, pp. 2440–2445.

Liu, X., Liu, L., Shao, Y., Zhao, Q., Zhang, Q., Lou, L., 2018. Water detection in urban areas from GF-3. Sensors 18 (4), 1299.

Martinis, S., Kersten, J., Twele, A., 2015. A fully automated Terrasar-X based flood service. ISPRS J. Photogramm. 104, 203–212 2013.

Martinis, S., Rieke, C., 2015. Backscatter analysis using multi-temporal and multi-frequency SAR data in the context of flood mapping at river Saale, Germany. Rem. Sens. 7 (6), 7732–7752.

Moreno, H.A., Vivoni, E.R., Gochis, D.J., 2013. Limits to flood forecasting in the Colorado front range for two summer convection periods using Radar nowcasting and a distributed hydrologic model. J. Hydrometeorol. 14 (4), 1075–1097.

Mueller, N., Lewis, A., Roberts, D., Ring, S., Melrose, R., Sixsmith, J., Lymburner, L., Mcintyre, A., Tan, P., Curnow, S., 2016. Water observations from space: mapping surface water from 25 years of Landsat imagery across Australia. Remote Sens. Environ. 174, 341–352.

Pekel, J.F., Cottam, A., Gorelick, N., Belward, A.S., 2016. High-resolution mapping of global surface water and its long-term changes. Nature 540 (7633), 418–422.

Poser, K., Dransch, D., 2010. Volunteered geographic information for disaster management with application to rapid flood damage estimation. Geomatica 64 (1), 89–98.

Reager, J., Famiglietti, J., 2009. Global terrestrial water storage capacity and flood potential using GRACE. Geophys. Res. Lett. 36 (23), L23402.

Revillaromero, B., Thielen, J., Salamon, P., De Groeve, T., Brakenridge, G.R., 2014. Evaluation of the satellite-based global flood detection system for measuring river discharge: influence of local factors. Hydrol. Earth Syst. Sci. 11 (11), 4467–4484.

Schlaffer, S., Matgen, P., Hollaus, M., Wagner, W., 2015. Flood detection from multi-temporal SAR data using harmonic analysis and change detection. Int. J. Appl. Earth Obs. 38, 15–24.

Sghaier, M.O., Hammami, I., Foucher, S., Lepage, R., 2018. Flood extent mapping from time-series SAR images based on texture analysis and data fusion. Rem. Sens. 10 (2), 237.

Shi, H., Li, T., Liu, R., Chen, J., Li, J., Zhang, A., Wang, G., 2015. A service-oriented architecture for ensemble flood forecast from numerical weather prediction. J. Hydrol. 527, 933–942.

Simonis, I., Echterhoff, J., 2006. Draft OpenGIS® Web Notification Service Implementation Specification (Version: 0.0.9). OGC Document Number: 06-095. Open Geospatial Consortium, Wayland, MA, USA.

Tong, X., Luo, X., Liu, S., Xie, H., Chao, W., Liu, S., Liu, S., Makhinov, A.N., Makhinova, A.F., Jiang, Y., 2018. An approach for flood monitoring by the combined use of Landsat 8 optical imagery and Cosmo-skymed radar imagery. ISPRS J. Photogramm. 136, 144–153.

Veh, G., Korup, O., Roessner, S., Walz, A., 2018. Detecting Himalayan glacial lake outburst floods from Landsat time series. Remote Sens. Environ. 207, 84–97.

Witherow, M.A., Elbakary, M.I., Iftekharuddin, K.M., Cetin, M., 2017. Analysis of crowdsourced images for flooding detection. European Congress on Computational Methods in Applied Sciences and Engineering. pp. 140–149.

Zhang, X., Chen, N., Chen, Z., Wu, L., Li, X., Zhang, L., Di, L., Gong, J., Li, D., 2018. Geospatial sensor web: a cyber-physical infrastructure for geoscience research and application. Earth Sci. Rev. 185, 684–703.